RESEARCH PAPER

Synthesis and Characterization of Nano-Structure Copper Oxide from Two Different Copper (II) Metal-Organic Framework Precursors

***Nadia Nasihatsheno** **

Department of Chemistry, Faculty of Sciences, Lorestan University, Khoramabad, Iran

ARTICLE INFO

Article History:
Received 14 February 2019
Accepted 26 April 2019
Published 15 June 2019

Keywords:
Metal-organic frameworks
CuO
Thermal decomposition
Nano-materials

ABSTRACT

Nano-structured copper oxides were successfully prepared through direct calcination of 1D ladder-like metal-organic framework $[Cu_2(btec)(2,2'\text{-bipy})_2]_\infty$, (btec = 1,2,4,5-benzenetetracarboxylate and 2,2'-bipy = 2,2'-bipyridine) and porous coordination polymer [Cu(BDC)(bipy)] ($BDCH_2$), (BDC = 1,4-benzenedicarboxylate; bipy = 4,4'-bipyridine). The nanostructure of the as-synthesized samples was characterized by X-ray powder diffraction (PXRD), Energy dispersive X-ray microanalysis (EDX) and scanning electron microscopy (SEM). Different reaction conditions were discussed. This study demonstrates the metal-organic frameworks may be adequate precursors for the preparation of nanoscale materials with different and remarkable morphologies.

How to cite this article
Nasihatsheno N. Synthesis and Characterization of Nano-Structure Copper Oxide from Two Different Copper (II) Metal-Organic Framework Precursors. Nanochem Res, 2019; 4(1):94-100. DOI: 10.22036/ncr.2019.01.011

INTRODUCTION

Metal-organic frameworks (MOFs) provide an intriguing way to design hybrid materials from organic linkers and metal ions and have attracted considerable attention because of their glamorous structures and potential applications in materials science and industrial technologies [1–4] including gas storage [5–7], separation [8–10], catalysis [11–13], magnetic resonance imaging (MRI) [14–17] and drug delivery [18–21]. Meanwhile, powders constituted by metal oxides are suitable products for the inorganic chemical industries. They find application in the fields of adsorption technology [22,23], heterogeneous catalysis [24], pigments technology [25] and as precursors for sintered ceramics [26]. Cupric oxide (CuO) is one of the most popular p-type semiconductor oxides, with a narrow band gap of 1.2 eV, that has been widely studied for a number of remarkable properties that can be used as heterogeneous catalysts in many significant chemical processes [24,27], as gas sensors [28,29], as a cathode material for electrochemical applications [30,31] and dye-sensitized solar cells [32,33]. So far, various nanostructured CuO crystals have been successfully synthesized through various methods such as sonochemical methods [34,35], double-jet precipitation methods [36,37], templating methods [38], precipitation [39], and wet-chemical methods [40,41]. The present work describes a facile route for preparation of CuO nanostructures by direct pyrolysis of two different Cu(II) metal-organic frameworks, $[Cu_2(btec)(2,2'\text{-bipy})_2]_\infty$ (**1**), and [Cu(BDC)(bipy)]($BDCH_2$) (**2**), as precursors under air atmosphere. The resulting nanomaterials were characterized by means of powder X-ray diffraction (PXRD), scanning electron microscopy (SEM), and energy dispersive X-ray microanalysis (EDX).

MATERIALS AND METHODS

All the ligands and transition metal salts were obtained commercially and used as received. X-ray powder diffraction patterns were measured using a Philips PW1800 powder diffractometer for Cu-K_α (λ = 0.17887 Å) with a scan speed of 1 s/step and a step size of 0.04°. The samples were characterized with a scanning electron microscope (SEM) (Hitachi

* Corresponding Author Email: *nadia.nshe@gmail.com*

S4160 and Philips XL30) with gold coating. Energy-dispersive X-ray analysis (EDX) was used to fulfill elemental microanalysis with a Philips XL30 operating at 17.0 kV.

Synthesis of [Cu_2(btec)(2,2'-bipy)$_2$]$_\infty$ (1)

[Cu_2(btec)(2,2'-bipy)$_2$]$_\infty$ (**1**) was synthesized by the method according to the literature [42]. In a typical synthesis of **1**, a mixture of $Cu(OAc)_2{\cdot}2H_2O$, H_4btec, NaOH, 2,2'-bipy, and H_2O with the molar ratio of 0.6:0.3:1.2:0.6:399.6 was stirred for 30 min, sealed in a Teflon-lined stainless steel autoclave and heated at 120 ˚C for 2 days. After cooling to room temperature, the dark blue powder product of **1** was collected.

Synthesis of [Cu(BDC)(bipy)](BDCH_2) (2)

Compound [Cu(BDC)(bipy)](BDCH_2) (**2**) was prepared using the reported method [43]. A mixture of $Cu(NO_3)_2$. $2.5H_2O$ (0.725 g, 0.3 mmol), $BDCH_2$ (0.05 g, 0.3 mmol), bipy (0.047 g, 0.3 mmol), and H_2O (3 ml) was heated in a Teflon-lined autoclave at 150 ˚C for 2 days and then cooled to room temperature. The blue powder product was filtered, washed with H_2O and ethanol, and air-dried to give [Cu(BDC)(bipy)](BDCH_2).

Synthesis of copper oxide nanoparticles

The precursors **1** and **2** were placed in a ceramic boat separately and calcinated in the furnace at 500 ˚C for 4 h under air atmosphere. After cooling at room temperature, black products were collected. Calcination at other temperatures (400 and 600 ˚C) followed the same process above.

RESULTS AND DISCUSSION

The structure of compounds [Cu_2(btec)(2,2'-bipy)$_2$]$_\infty$ (**1**) and [Cu(BDC)(bipy)](BDCH_2) (**2**)

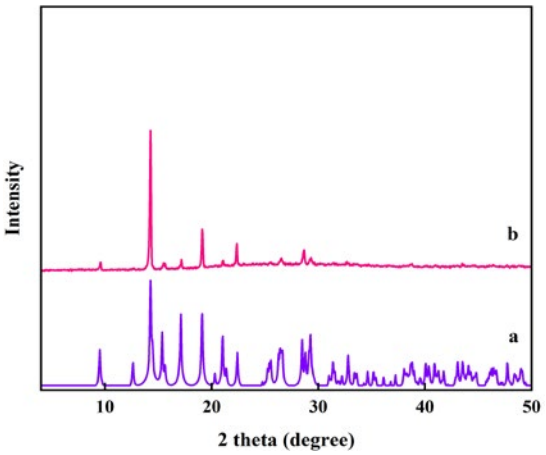

Fig. 1. X-ray powder pattern of [Cu_2(btec)(2,2'-bipy)$_2$]$_\infty$ MOF. (a) The simulated pattern of single crystal X-ray data and (b) experimental pattern of as-synthesized MOF.

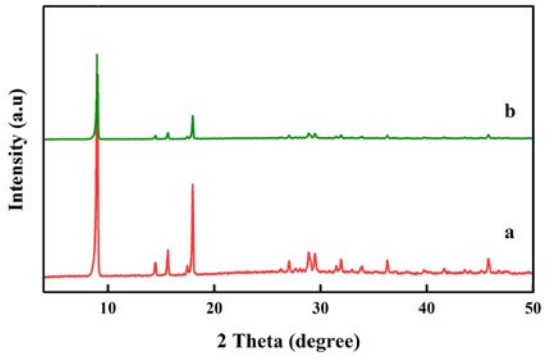

Fig. 2. Powder X-ray diffraction patterns for [Cu(BDC)(bipy)](BDCH_2) analogs; (a) the original form, (b) as synthesized.

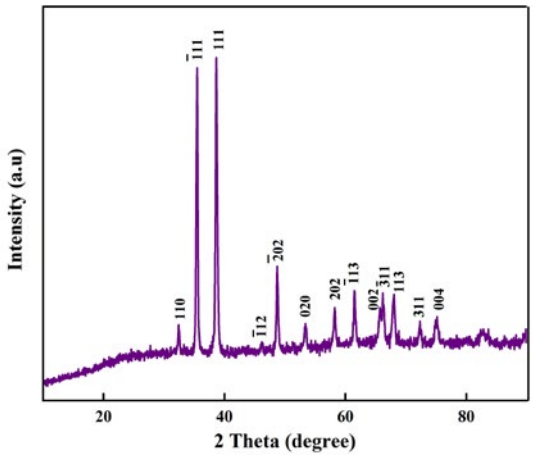

Fig. 3. PXRD pattern of as-synthesized CuO product by in-situ calcination of [Cu_2(btec)(2,2'-bipy)$_2$]$_\infty$ at 500 ˚C for 4 h.

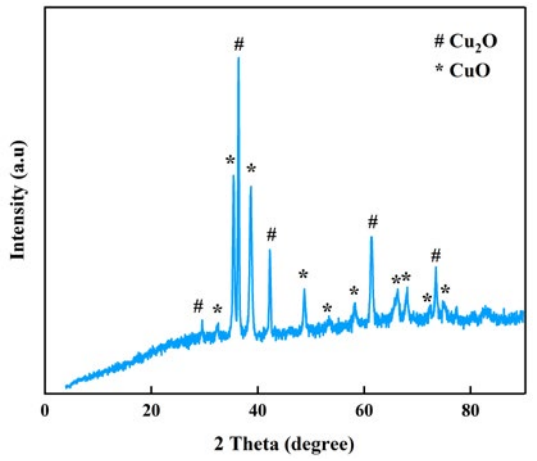

Fig. 4. PXRD pattern resulting from calcination of the [Cu(BDC)(bipy)](BDCH_2) MOF at 500 ˚C.

were previously analyzed and reported [42,43]. The simulated diffraction pattern of the reflections of the single crystal diffraction agrees with the experimental PXRD pattern of the formed powder MOFs, as shown in Figs. 1 and 2, respectively. In this study, CuO nanostructures were simply synthesized by direct calcination of the Cu-MOFs at 500 ˚C under air atmosphere without using any additional reducing agent or template. The crystalline structures and phase purity of as-synthesized products were first examined by PXRD with the results shown in Figs. 3 and 4, respectively. Fig. 3 shows the crystal structure of product resulted from **1** is corresponding to copper(II) oxide (CuO) (Tenorite; S.G.: C2/c; cell parameters: a = 4.685; b = 3.23; c = 5.132; β = 99.52; JCPDS file no. 41-0254). No peaks of other phases can be found, indicating that a pure product was obtained. Also, the peak positions appeared from **2** corresponding to a mixture of Cu_2O (Cuprite; S.G.: Pn3m; with lattice constant a = 4.269; JCPDS file no. 05-0667) and CuO (Tenorite; JCPDS file no. 41-0254) in major phase, as shown in Fig. 4. Furthermore, the EDX spectra at 600 ˚C in Figs. 5 and 6 demonstrate that copper oxide is generated. The morphology and sizes of as-synthesized

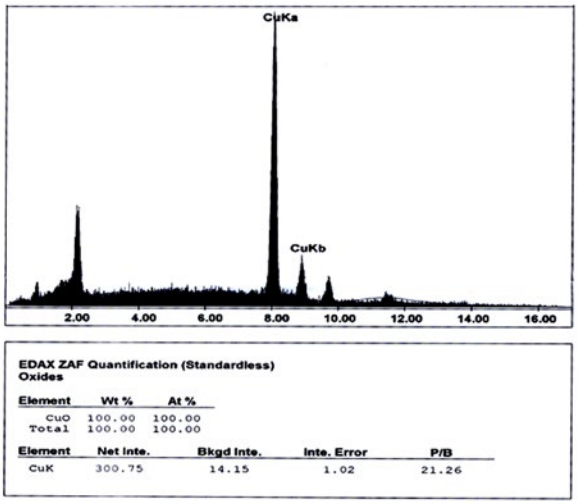

Fig. 5. EDX spectrum of the as-synthesized product by calcination of $[Cu_2(btec)(2,2'\text{-bipy})_2]_\infty$ MOF at 600 ˚C for 4 h in the air.

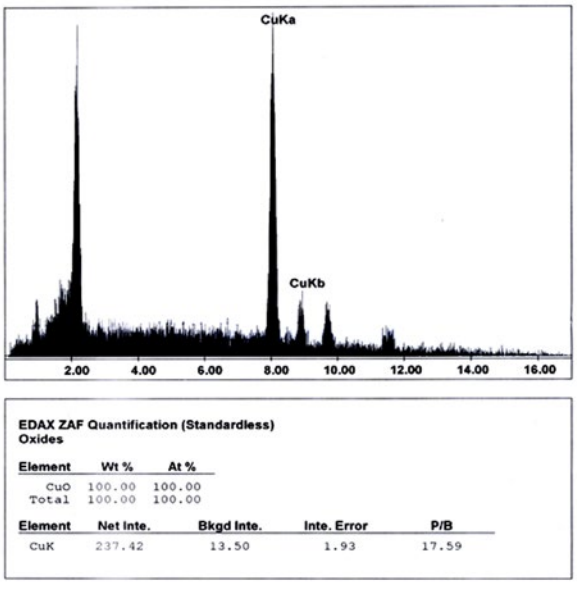

Fig. 6. EDX spectrum of as-synthesized products by calcination of the [Cu(BDC)(bipy)]$(BDCH_2)$ at 600 ˚C for 4 h.

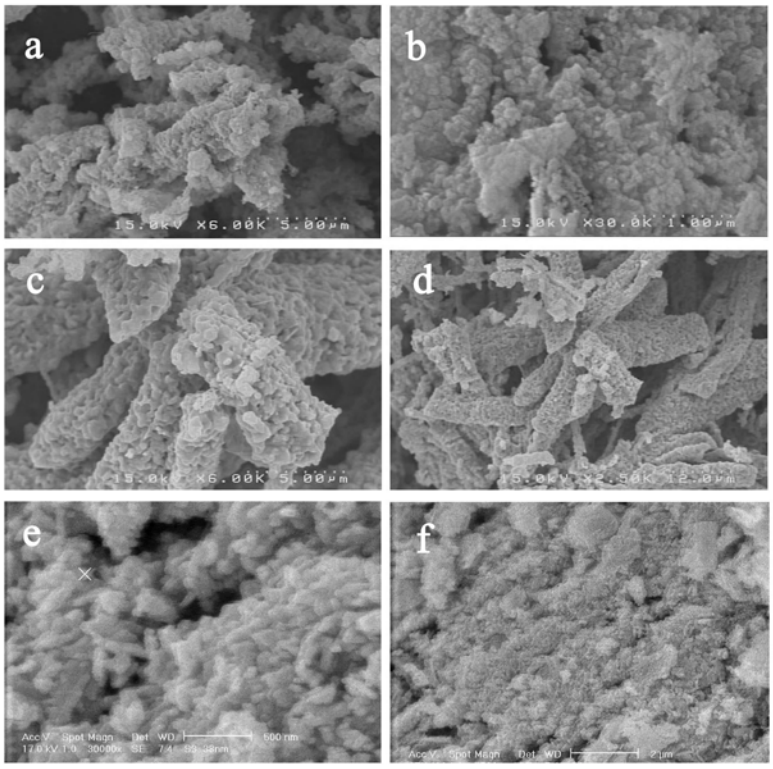

Fig. 7. SEM photographs of CuO nanostructure produced by calcination of $[Cu_2(btec)(2,2'\text{-bipy})_2]_\infty$ MOF for 4 h in the air, (a-b) at 400, (c-d) 500, and (e-f) 600 ˚C, respectively.

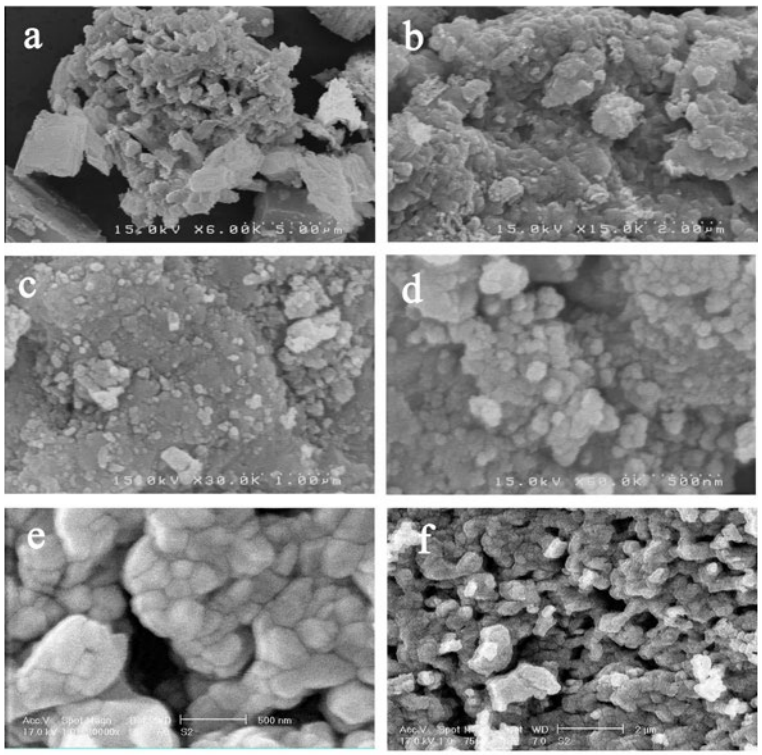

Fig. 8. Surface morphology (SEM image) of as-prepared [Cu(BDC)(bipy)]($BDCH_2$) MOF after calcination at 400 (a-b), 500 (c-d), and 600˚C (e-f), respectively.

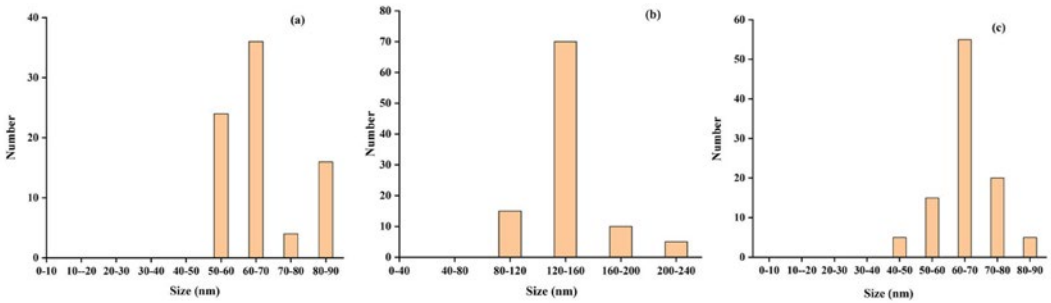

Fig. 9. Particle size histogram of CuO nanoparticles for $[Cu_2(btec)(2,2'\text{-bipy})_2]_\infty$ MOF at 400 (a), 500 (b) and 600 ˚C (c).

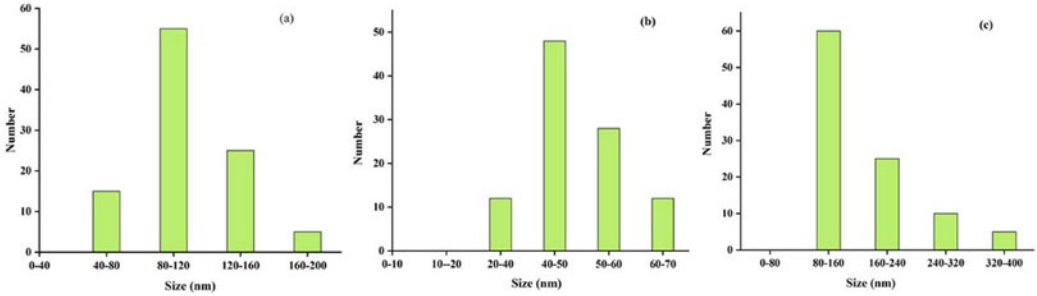

Fig. 10. Particle size histogram of CuO nanoparticles for $[Cu(BDC)(bipy)](BDCH_2)$ MOF at 400 (a), 500 (b) and 600 ˚C (c).

copper oxide products were further characterized by SEM. Reaction conditions have a large effect on the final products. To investigate the role of reaction temperature on the final products during calcination of the Cu-MOFs under air atmosphere, we further studied the morphology and particle size of the final products by calcination of the Cu-MOFs at different reaction temperatures varying from 400 to 600 ˚C for 4 h, (Figs. 7-8). So, we can see that with the variation of reaction temperature, copper oxide nanoparticles can be generated, but with different morphologies. As shown from histogram in Fig. 9 (a-c), the particles size was obtained 65, 140, and 65 nm, respectively, at 400, 500, and 600 ˚C for **1**, and the formed nanoparticles from **2** have a diameter about 100, 45 and 120 nm at 400, 500 and 600 ˚C, respectively (Fig. 10 (a-c))**.**

CONCLUSION

In summary, we have explained the successful preparation of copper oxide nanoparticles by direct calcination of the 1D ladder-like $[Cu_2(btec)(2,2'\text{-bipy})_2]_\infty$ metal-organic framework and porous coordination polymer $[Cu(BDC)(bipy)](BDCH_2)$ under air atmosphere. Calcination temperature has a great effect on the size and shape of the final products. The variation of reaction temperature from 400 to 600 ˚C led to the different particle sizes and morphologies of copper oxide nanoparticles. This process builds a direct relation between metal-carboxylate MOF crystals and metal oxide nanostructures and further opens a new application field for MOFs.

ACKNOWLEDGMENTS

This work was supported by the Lorestan University.

CONFLICT OF INTEREST

The author declared to no conflict of interest.

REFERENCES

[1] Tranchemontagne DJ, Mendoza-Cortés JL, O'Keeffe M, Yaghi OM. Secondary building units, nets and bonding in the chemistry of metal–organic frameworks. Chemical Society Reviews. 2009;38(5):1257.

[2] Silva P, Vilela SMF, Tomé JPC, Almeida Paz FA. Multifunctional metal–organic frameworks: from academia to industrial applications. Chemical Society Reviews. 2015;44(19):6774-803.

[3] Czaja AU, Trukhan N, Müller U. Industrial applications of metal–organic frameworks. Chemical Society Reviews. 2009;38(5):1284.

[4] Ajoyan Z, Marino P, Howarth AJ. Green applications of metal–organic frameworks. CrystEngComm. 2018;20(39):5899-912.

[5] Rowsell JLC, Millward AR, Park KS, Yaghi OM. Hydrogen Sorption in Functionalized Metal–Organic Frameworks. Journal of the American Chemical Society. 2004;126(18):5666-7.
[6] Li H, Wang K, Sun Y, Lollar CT, Li J, Zhou H-C. Recent advances in gas storage and separation using metal–organic frameworks. Materials Today. 2018;21(2):108-21.
[7] Li B, Wen H-M, Zhou W, Chen B. Porous Metal–Organic Frameworks for Gas Storage and Separation: What, How, and Why? The Journal of Physical Chemistry Letters. 2014;5(20):3468-79.
[8] Lin R-B, Xiang S, Xing H, Zhou W, Chen B. Exploration of porous metal–organic frameworks for gas separation and purification. Coordination Chemistry Reviews. 2019;378:87-103.
[9] Kang Z, Fan L, Sun D. Recent advances and challenges of metal–organic framework membranes for gas separation. Journal of Materials Chemistry A. 2017;5(21):10073-91.
[10] Li Z, Hüve J, Krampe C, Luppi G, Tsotsalas M, Klingauf J, et al. Internalization Pathways of Anisotropic Disc-Shaped Zeolite L Nanocrystals with Different Surface Properties in HeLa Cancer Cells. Small. 2013;9(9-10):1809-20.
[11] Ranocchiari M, Bokhoven JAv. Catalysis by metal–organic frameworks: fundamentals and opportunities. Physical Chemistry Chemical Physics. 2011;13(14):6388.
[12] Zhu L, Liu X-Q, Jiang H-L, Sun L-B. Metal–Organic Frameworks for Heterogeneous Basic Catalysis. Chemical Reviews. 2017;117(12):8129-76.
[13] Dhakshinamoorthy A, Li Z, Garcia H. Catalysis and photocatalysis by metal organic frameworks. Chemical Society Reviews. 2018; 47(22): 8134-72.
[14] Liu D, Lu K, Poon C, Lin W. Metal–Organic Frameworks as Sensory Materials and Imaging Agents. Inorganic Chemistry. 2013;53(4):1916-24.
[15] Hatakeyama W, Sanchez TJ, Rowe MD, Serkova NJ, Liberatore MW, Boyes SG. Synthesis of Gadolinium Nanoscale Metal–Organic Framework with Hydrotropes: Manipulation of Particle Size and Magnetic Resonance Imaging Capability. ACS Applied Materials & Interfaces. 2011;3(5):1502-10.
[16] Taylor KML, Rieter WJ, Lin W. Manganese-Based Nanoscale Metal–Organic Frameworks for Magnetic Resonance Imaging. Journal of the American Chemical Society. 2008;130(44):14358-9.
[17] Peller M, Böll K, Zimpel A, Wuttke S. Metal–organic framework nanoparticles for magnetic resonance imaging. Inorganic Chemistry Frontiers. 2018;5(8):1760-79.
[18] Zheng H, Zhang Y, Liu L, Wan W, Guo P, Nyström AM, et al. One-pot Synthesis of Metal–Organic Frameworks with Encapsulated Target Molecules and Their Applications for Controlled Drug Delivery. Journal of the American Chemical Society. 2016;138(3):962-8.
[19] Orellana-Tavra C, Marshall RJ, Baxter EF, Lázaro IA, Tao A, Cheetham AK, et al. Drug delivery and controlled release from biocompatible metal–organic frameworks using mechanical amorphization. Journal of Materials Chemistry B. 2016;4(47):7697-707.
[20] Wu M-X, Yang Y-W. Metal-Organic Framework (MOF)-Based Drug/Cargo Delivery and Cancer Therapy. Advanced Materials. 2017;29(23):1606134.
[21] Sun C-Y, Qin C, Wang X-L, Su Z-M. Metal-organic frameworks as potential drug delivery systems. Expert Opinion on Drug Delivery. 2012;10(1):89-101.
[22] Hua M, Zhang S, Pan B, Zhang W, Lv L, Zhang Q. Heavy metal removal from water/wastewater by nanosized metal oxides: A review. Journal of Hazardous Materials. 2012;211-212:317-31.
[23] Hu J-S, Zhong L-S, Song W-G, Wan L-J. Synthesis of Hierarchically Structured Metal Oxides and their Application in Heavy Metal Ion Removal. Advanced Materials. 2008;20(15):2977-82.
[24] Wang Y, Arandiyan H, Scott J, Bagheri A, Dai H, Amal R. Recent advances in ordered meso/macroporous metal oxides for heterogeneous catalysis: a review. Journal of Materials Chemistry A. 2017;5(19):8825-46.
[25] Fouad OA, Hassan AM, Abd El-Wahab H, Mohy Eldin A, Naser A-RM, Wahba OAG. Synthesis, characterization and application of some nanosized mixed metal oxides as high heat resistant pigments: Ca2CuO3, Ca3Co2O6, and NiSb2O6. Journal of Alloys and Compounds. 2012;537:165-70.
[26] Komarneni S, Roy R, Li QH. Microwave-hydrothermal synthesis of ceramic powders. Materials Research Bulletin. 1992;27(12):1393-405.
[27] Gawande MB, Pandey RK, Jayaram RV. Role of mixed metal oxides in catalysis science—versatile applications in organic synthesis. Catalysis Science & Technology. 2012;2(6):1113.
[28] Dey A. Semiconductor metal oxide gas sensors: A review. Materials Science and Engineering: B. 2018;229:206-17.
[29] Wang C, Yin L, Zhang L, Xiang D, Gao R. Metal Oxide Gas Sensors: Sensitivity and Influencing Factors. Sensors. 2010;10(3):2088-106.
[30] Desilvestro J. Metal Oxide Cathode Materials for Electrochemical Energy Storage: A Review. Journal of The Electrochemical Society. 1990;137(1):5C.
[31] Ratynski M, Hamankiewicz B, Krajewski M, Boczar M, Ziolkowska D, Czerwinski A. Single Step, Electrochemical Preparation of Copper-Based Positive Electrode for Lithium Primary Cells. Materials. 2018;11(11):2126.
[32] Shaikh JS, Shaikh NS, Mali SS, Patil JV, Pawar KK, Kanjanaboos P, et al. Nanoarchitectures in dye-sensitized solar cells: metal oxides, oxide perovskites and carbon-based materials. Nanoscale. 2018;10(11):4987-5034.
[33] Jose R, Thavasi V, Ramakrishna S. Metal Oxides for Dye-Sensitized Solar Cells. Journal of the American Ceramic Society. 2009;92(2):289-301.
[34] Wongpisutpaisan N, Charoonsuk P, Vittayakorn N, Pecharapa W. Sonochemical Synthesis and Characterization of Copper Oxide Nanoparticles. Energy Procedia. 2011;9:404-9.
[35] Ranjbar-Karimi R, Bazmandegan-Shamili A, Aslani A, Kaviani K. Sonochemical synthesis, characterization and thermal and optical analysis of CuO nanoparticles. Physica B: Condensed Matter. 2010;405(15):3096-100.
[36] Kobayashi Y, Yasuda Y, Morita T. Recent advances in the synthesis of copper-based nanoparticles for metal–metal bonding processes. Journal of Science: Advanced Materials and Devices. 2016;1(4):413-30.
[37] Lee S-H, Her Y-S, Matijević E. Preparation and Growth Mechanism of Uniform Colloidal Copper Oxide by the Controlled Double-Jet Precipitation. Journal of Colloid and Interface Science. 1997;186(1):193-202.
[38] Wu H-Q, Wei X-W, Shao M-W, Gu J-S, Qu M-Z. Synthesis of copper oxide nanoparticles using carbon nanotubes as templates. Chemical Physics Letters. 2002;364(1-2):152-6.
[39] Phiwdang K, Suphankij S, Mekprasart W, Pecharapa W. Synthesis of CuO Nanoparticles by Precipitation Method

Using Different Precursors. Energy Procedia. 2013;34:740-5.
[40] Tran TH, Nguyen VT. Copper Oxide Nanomaterials Prepared by Solution Methods, Some Properties, and Potential Applications: A Brief Review. International Scholarly Research Notices. 2014;2014:1-14.
[41] Xue B, Qian Z, Liu C, Luo G. Synthesis of CuO nanoparticles via one-pot wet-chemical method and its catalytic performance on the thermal decomposition of ammonium perchlorate. Russian Journal of Applied Chemistry. 2017;90(1):138-43.
[42] Hao N, Li Y, Wang E, Shen E, Hu C, Xu L. Hydrothermal synthesis and crystal structure of an infinite 1D ladderlike metal-organic compound: [Cu2(btec)(2,2′-bipy)2]∞ (btec=1,2,4,5-benzenetetracarboxylate). Journal of Molecular Structure. 2004;697(1-3):1-8.
[43] Baeg JY, Lee SW. A porous, two-dimensional copper coordination-polymer containing guest molecules: hydrothermal synthesis, structure, and thermal property of [Cu(BDC)(bipy)](BDCH 2) (BDC=1,4-benzenedicarboxylate; bipy=4,4 ′ -bipyridine). Inorganic Chemistry Communications. 2003;6(3):313-6.